Geophysical Research Letters

RESEARCH LETTER
10.1029/2021GL096527

Thirty Years of GOSHIP and WOCE Data: Atlantic Overturning of Mass, Heat, and Freshwater Transport

V. Caínzos[1], A. Hernández-Guerra[1], G. D. McCarthy[2], E. L. McDonagh[3,4], M. Cubas Armas[1], and M. D. Pérez-Hernández[1]

[1]Unidad Océano y Clima, Instituto de Oceanografía y Cambio Global, IOCAG, Universidad de Las Palmas de Gran Canaria, ULPGC, Unidad Asociada ULPGC-CSIC, Canary Islands, Spain, [2]ICARUS, Department of Geography, Maynooth University, Maynooth, Ireland, [3]NORCE Norwegian Research Centre, Bjerknes Centre for Climate Research, Bergen, Norway, [4]National Oceanography Centre (NOC), Southampton, UK

Key Points:

- No changes at any latitude between hydrographic sections carried out in the last 30 years
- The major contributor to the Atlantic Meridional Overturning Circulation at the subpolar North Atlantic is the Eastern subbasin for the three decades
- The increase of southward freshwater overturning transport at 30°S indicates a bistable state of the AMOC

Supporting Information:

Supporting Information may be found in the online version of this article.

Correspondence to:

V. Caínzos,
veronica.cainzos@ulpgc.es

Citation:

Caínzos, V., Hernández-Guerra, A., McCarthy, G. D., McDonagh, E. L., Cubas Armas, M., & Pérez-Hernández, M. D. (2022). Thirty years of GOSHIP and WOCE data: Atlantic overturning of mass, heat, and freshwater transport. *Geophysical Research Letters*, *49*, e2021GL096527. https://doi.org/10.1029/2021GL096527

Received 13 OCT 2021
Accepted 31 JAN 2022

Abstract The Atlantic Meridional Overturning Circulation (AMOC) plays a vital role in global climate, redistributing heat, and freshwater. It is predicted to decline due to anthropogenic climate change, with major implications for global climate. Accurately assessing AMOC strength with in situ observations has inspired a number of dedicated observing systems in the Atlantic since the 2000s. However, no consensus has been reached on whether the slowdown of the AMOC and its associated heat and freshwater transports is occurring. These dedicated systems are too recent to detect long-term trends. We have analyzed hydrographic data from zonal sections across the Atlantic for 30 years that predate and overlap the era of AMOC observations. Our results show no changes in the AMOC for all sections analyzed over the whole Atlantic for the last 30 years. We also find an increased export of freshwater from the South Atlantic associated with an increase in upper salinity.

Plain Language Summary The Atlantic Meridional Overturning Circulation (AMOC) is the oceanic process by which upper warm waters flow northward and cold deep waters flow southward. The AMOC has a large effect on European and global climate. Models have predicted a decline of its strength due to anthropogenic climate change. Across-ocean systems monitoring the currents on the water column have yet to find this slowdown. We have analyzed hydrographic data collected for the last 30 years and have built a model for each decade of the circulation of the Atlantic, and found no changes in time in the Atlantic Ocean for each hydrographic section. Also, our results present an increase in the amount of freshwater leaving the South Atlantic.

1. Introduction

The Atlantic Meridional Overturning Circulation (AMOC) transports relatively warm surface, thermocline, and intermediate waters northwards. This warm upper limb of the overturning circulation releases heat to the atmosphere on its way northward, loses buoyancy, and eventually sinks in the subpolar North Atlantic (SPNA) and Nordic Seas, returning south as North Atlantic Deep Water (NADW; Srokosz et al., 2012). Recent publications have addressed the long-term millennial evolution of the AMOC and suggest that it has been in a relative weak state in recent decades (Caesar et al., 2021). AMOC also varies on timescales from seasonal to decadal (Desbruyères et al., 2019; Moat et al., 2020; Sévellec & Sinha, 2018).

A great effort to sample the global ocean has been carried out since the 1990s under the World Ocean Circulation Experiment (WOCE) and, later, the GO-SHIP (Talley et al., 2016) programs. As a result, a global network of zonal and meridional transoceanic hydrographic sections is available, with repetitions every 5–10 years. The WOCE hydrographic cruises enabled the computation of a global ocean linear inverse box model for the 1990s focused on estimating the transports of mass, heat, and freshwater in every ocean (Ganachaud & Wunsch, 2000, 2003), thus creating a consistent picture of the global ocean circulation.

The need for further information about the evolution of the AMOC led to the deployment of several mooring arrays in key latitudes to continuously measure the AMOC. The OSNAP (Lozier et al., 2017), RAPID/MOCHA/WBTS array (hereafter the RAPID array; Cunningham et al., 2007; Johns et al., 2011), MOVE (Kanzow et al., 2006), TSAA (Hummels et al., 2015), and SAMBA (Meinen et al., 2013) projects in the Atlantic Ocean have measured the overturning transport variability on timescales of days, months, or seasons (Frajka-Williams et al., 2019; McCarthy et al., 2020). However, with the earliest results dating the 2000s, these mooring arrays

cannot address the longer term decadal changes in the Atlantic Ocean. Hydrographic data, therefore, offer the only opportunity to understand longer term subsurface variability. Thus, different studies have compared hydrographic sections conducted at different times, to determine changes of these transports at selected latitudes (Baringer & Molinari, 1999; Bryden et al., 2005; Fu et al., 2018; Hernández-Guerra & Talley, 2016; Hernández-Guerra et al., 2014, 2019; Koltermann et al., 1999; McDonagh et al., 2015).

2. Materials and Methods

We have constructed three inverse models in a neutral density (Jackett & McDougall, 1997) framework, one for each of the last three decades, using hydrographic data for the entire Atlantic Ocean. The latitudinal configuration in each decade varies depending on the available transoceanic sections.

2.1. Hydrographic Data

Basinwide, zonal sections, collected since the 1990s, are part of a collective effort to characterize the ocean in the frame of the international GO-SHIP Program (Talley et al., 2016).

We have prioritized the repeated zonal sections for each decade in our study (Figure 1), which are: 55°N (AR07W + AR07E), 24°N (A05), and 30°S (A10). Table S1 in Supporting Information S1 summarizes the chosen sections and their characteristics.

Atlantic water masses are identified with potential temperature, salinity, and neutral density (γ^n) vertical sections (Figure S1 in Supporting Information S1), which allow defining the reference layer for each section to be used in the thermal wind equation to estimate the geostrophic velocities and transports. The level of no motion is set at the interphase of water masses with different directions, such as the southward NADW and the northward Antarctic Bottom Water (AABW). To compute the mass transports, the water column is divided into several γ^n layers (Hernández-Guerra et al., 2019; Talley, 2008). Additionally, the surface Ekman transport at the time of the cruise is estimated using the NCEP–NCAR surface winds.

2.2. Inverse Box Model

The estimated mass transport is not balanced with its adjacent hydrographic sections, as the assumed level of no motion has indeed a velocity different from zero. Thus, inverse box models were introduced in oceanography to estimate the unknown geostrophic reference velocities for hydrographic station pairs, subject to chosen constraints and uncertainties, the most basic of which is mass conservation (Wunsch, 1978, 1996). Conservation of mass is imposed for each box for the whole water column and each layer. For every single section, mass is conserved for regional constraints, related to independent in situ measurements and topographic features. The salinity content of each section is also constrained (Tables S3, S4 and S5 in Supporting Information S1) to make sure that mass is conserved while allowing changes in freshwater. The Gauss-Markov estimator is applied to solve these matrices (Wunsch, 1996). The same model configuration is used for each decade, so that differences in the model solution are attributable to changes in circulation.

3. Results and Discussion

3.1. Meridional Transport

Two counter-rotating overturning cells appear in the results of the inverse models (background arrows in Figure 2). The upper overturning cell is partially closed by the vertical transport of water, with downward vertical transport in the SPNA associated with entrainment of warm North Atlantic Current (NAC; McCartney & Talley, 1984) and upwelling in the subtropical gyre of the South Atlantic Ocean (Figure 2). In the abyssal cell, part of the southward flowing NADW sinks in the Southern Ocean and then returns northward as the AABW (Wefer et al., 1996) that then upwells on its way north to the subtropical North Atlantic. This study does not reach latitudes south enough to observe the deep-water formation in the Southern Ocean. The northward transports of upper and abyssal layers are balanced by the southward transport of deep layers (Kersalé et al., 2020). The boundaries of the deep layers lie between γ^n of 27.84 and 28.15 kg m^{-3} for the southern hemisphere and between or 27.58 and 28.15 kg m^{-3} or bottom for the northern hemisphere.

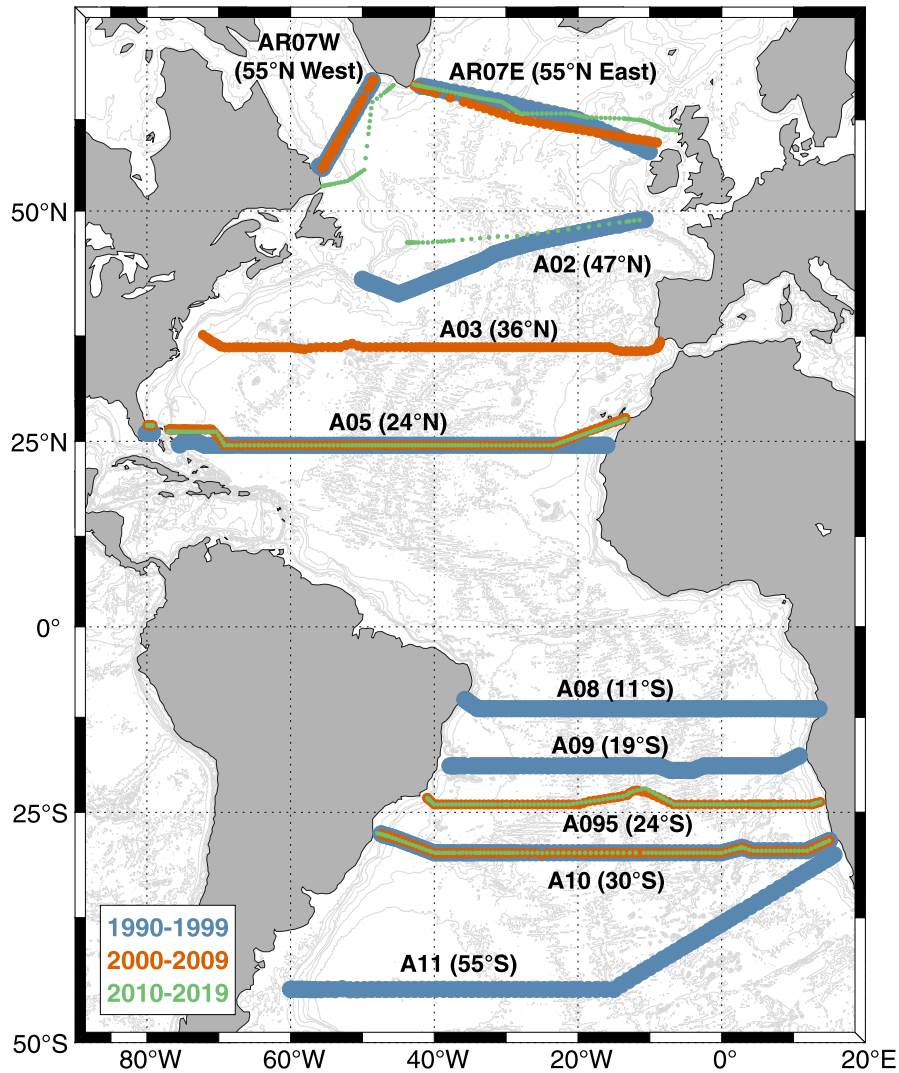

Figure 1. Map of the zonal sections included in each decade for the inverse model. Each section is accompanied by its World Ocean Circulation Experiment name and its nominal latitude (between parenthesis) and the colors represent each decade, blue for 1990–1999, orange for 2000–2009, and green for 2010–2019. Three sections have been repeated in every decade (A10 – 30°S, A05 – 24°N, AR07W and AR07E – 55°N).

In the SPNA, the core of the warm NAC gets denser on its way northward, as seen in sections 47°N and 55°N (Figure 2), with stronger northward transports between γ^n of 26.45 and 27.58 kg m^{-3} at 47°N (12.4 ± 1.8 Sv for 1990–1999 and 13.7 ± 1.5 Sv for 2010–2019) and between γ^n of 27.23 and 27.84 kg m^{-3} at 55°N (12.1 ± 2.5 Sv for 1990–1999, 11.0 ± 1.9 Sv for 2000–2009 and 11.6 ± 1.7 Sv for 2010–2019, where 1 Sverdrup (Sv) = 10^6 m^3 s^{-1} ≈ 10^9 kg s^{-1}). This maximum is associated with stronger downwelling values at 27.00–27.84 kg m^{-3}.

In the thermocline layers of the subtropical regions of both hemispheres (sections 24°S, 19°S, 11°S, 24°N and 36°N) the transport is maximum at the surface, decreasing with depth, reflecting the usual structure of a wind-driven subtropical gyre. The apparent variability in the horizontal and vertical fluxes observed in Figure 2 could be due to the different latitudinal extent among sections in the different decades.

3.2. Overturning Circulation

The meridional overturning circulation is evident in the section-average net transport of northward water by the upper and abyssal layers and by the southward transport by deep layers for all latitudes (Figure 3).

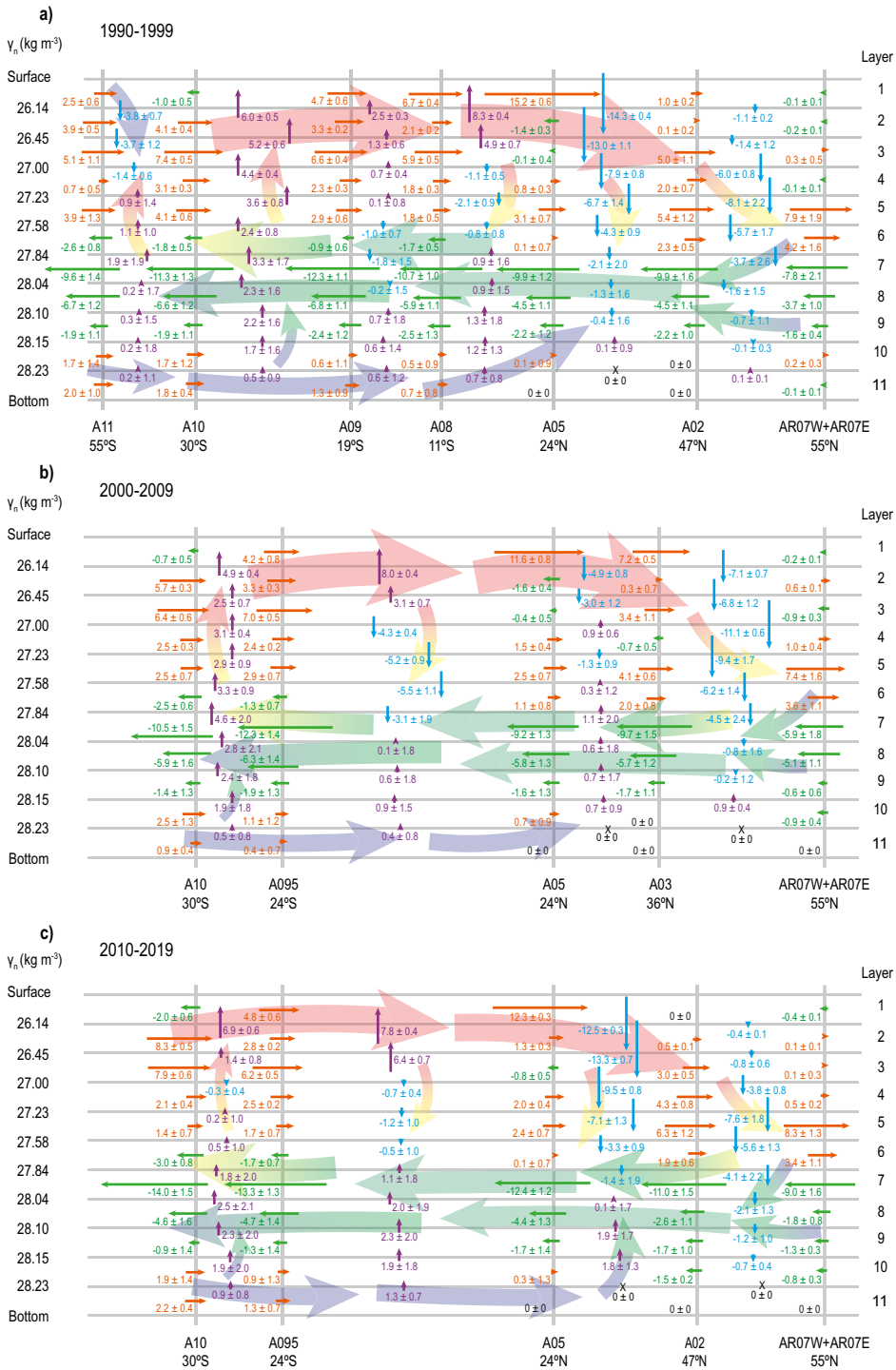

Figure 2. Vertical and meridional schematic of the circulation in the Atlantic Ocean for each decade. The gray horizontal lines mark the neutral density interphases, and the gray vertical lines are the position of each zonal section at their nominal latitude for the (a) 1990–1999 decade, (b) 2000–2009 decade, and (c) 2010–2019 decade. The horizontal mass transport (1 Sverdrup (Sv) = 10^6 m^3 s^{-1} ≈ 10^9 kg s^{-1}) is represented with horizontal arrows, in orange for northward (positive) transport and green for southward (negative) transport. Black dots in the North Atlantic appear in layers with null transport. The vertical transport between two sections in the interphase between two layers is represented with vertical arrows, in violet for upward (positive) transport and blue for downward (negative) transport. Black crosses represent layers with no vertical transport. The uncertainties associated with mass transport are part of the results of the inverse model using the Gauss-Markov estimator. Background arrows manifest the presence of two counter-rotating overturning cells across the basin. A consistent circulation through the decades is observed, with upwelling in the southern subtropical gyre and downwelling in the northern subtropical gyre and the subpolar North Atlantic.

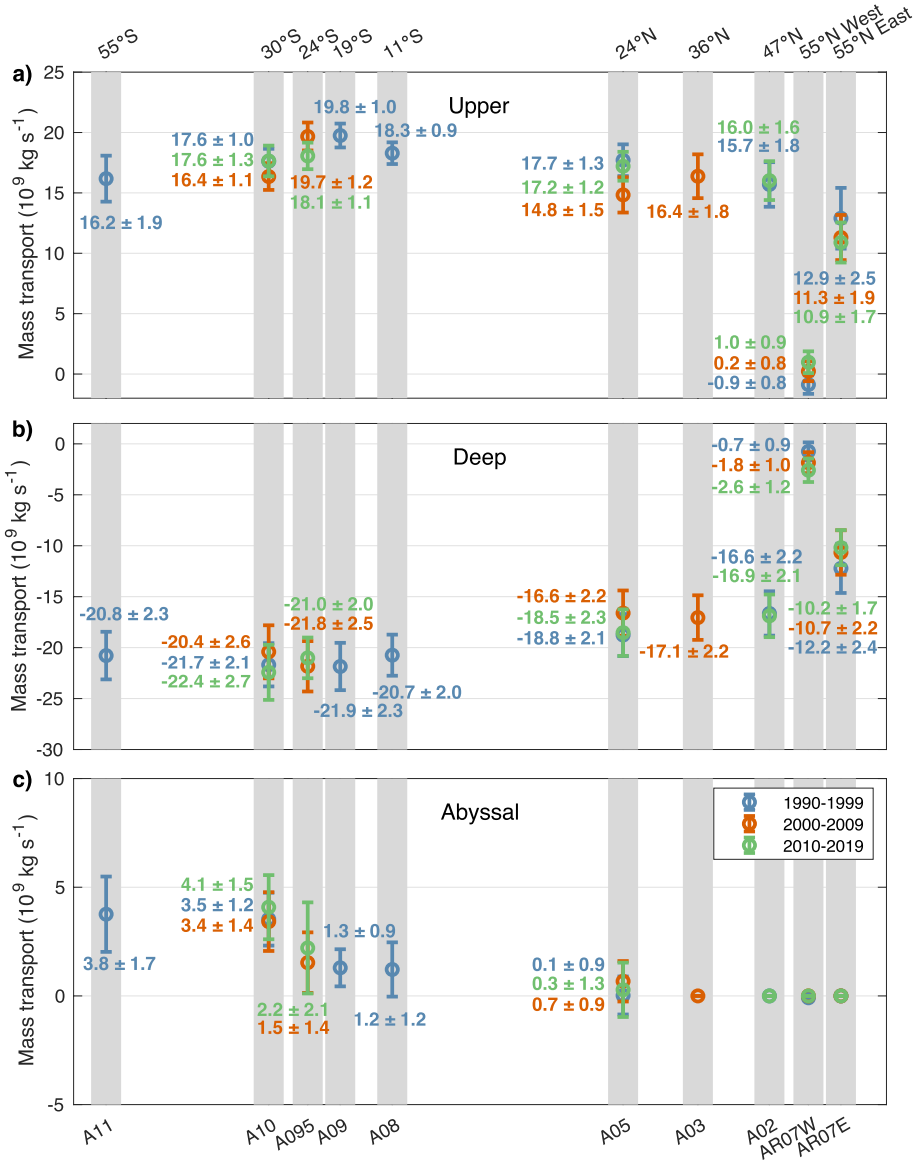

Figure 3. Mass transport (1 Sverdrup (Sv) = 10^6 m^3 s^{-1} ≈ 10^9 kg s^{-1}) attending to each layer for each latitude and decade. The gray bars mark the nominal latitude of each zonal section, and the colors represent each decade, blue for 1990–1999, orange for 2000–2009, and green for 2010–2019. The mass transport is divided into three layers – upper (a), deep (b), and abyssal (c). The interphases between these layers are defined as the change from north to south (south to north) transport for upper to deep (deep to bottom) layers in neutral density coordinates. The uncertainties associated with the mass transport are part of the results of the inverse model solved using the Gauss-Markov estimator.

There is no apparent change in the overturning strength among the diverse hydrographic realizations carried out in different decades, with no differences for the upper, deep, and abyssal layers across the Atlantic Ocean. However, we have to be aware that there are some limitations associated with inverse modeling of hydrographic data. Each inverse solution could be interpreted as representative of a relatively short time interval (Fu et al., 2020) or could give information of monthly variations of the AMOC (Bryden et al., 2005). Similarly, Ganachaud and Wunsch (2003) refer to their estimates as time-average transoceanic transports with realistic uncertainties, although they acknowledge the temporal sampling problem inherent to the discrete sampling of hydrographic data.

Our results are similar to those obtained by other inverse models of the Atlantic with data of the first decade of our study (Ganachaud, 2003b; Lumpkin & Speer, 2007; Macdonald, 1995; Sloyan & Rintoul, 2001; Table S2 in Supporting Information S1). In general, the results agree, but we find more differences in upper layers and our model

tends to provide smaller transports in bottom layers. A recent reconstruction of three decades of inverse models using sections north of 24°N (Fu et al., 2020) has also found stability in the strength of the AMOC for the SPNA.

OSNAP data products are available for 21 months, from July 2014 to March 2016 (Lozier et al., 2019). AMOC values from OSNAP data can be compared to those of the inverse model for the last decade of the section at 55°N (West and East) but taking into account the shorter period in OSNAP data and the limitation of the inverse model solutions described before. The mass transports from the inverse model for each subbasin (1.0 ± 0.9 Sv for the West and 10.9 ± 1.7 Sv for the East) are slightly weaker than those obtained by OSNAP (2.1 ± 0.3 Sv for the West and 15.6 ± 0.8 Sv for the East). However, for the total section, the subpolar AMOC is not different (11.9 ± 2.1 Sv for the inverse model and 14.9 ± 0.9 Sv for OSNAP). Our results indicate a fairly constant weak transport in the Labrador basin over the three decades, and the Eastern basin being the major contributor to the AMOC, evidencing the OSNAP findings (Lozier et al., 2019; Petit et al., 2020) of weak transport in the Labrador Sea between 2014 and 2016 that have persisted for the previous three decades.

AMOC estimates are also available for the RAPID program from April 2004 to August 2018 (Moat et al., 2020). Values for the 2010–2019 decade are very similar between the inverse model (24°N cruise in 2011) and RAPID (over 2010–2018) for upper (17.2 ± 1.2 and 16.4 ± 4.5 Sv, respectively), deep (-18.5 ± 2.3 and -17.3 ± 4.1 Sv, respectively) and abyssal (0.3 ± 1.3 and 1.1 ± 0.6 Sv, respectively) layers. The mass transports of the inverse model of the 2000-2009 decade (24°N cruise in 2004) are weaker than RAPID values (averaged over the interval 2004–2009) for upper (14.8 ± 1.5 and 18.0 ± 4.7 Sv, respectively), deep (-16.6 ± 2.2 and -18.6 ± 4.3 Sv, respectively), and abyssal (0.7 ± 0.9 and 0.8 ± 0.6 Sv, respectively), although not different, in part due to the high uncertainties associated to RAPID data.

The question of the slowing of the AMOC or not is exceptionally important. Contrasting the results of in situ observations and reconstructions is a significant contribution to the debate. Monitoring programs enabled the observation of interannual changes in AMOC, such as the 0.5 Sv/year weakening of the AMOC at 26.5°N between 2004 and 2012, possibly explained by internal variability (Roberts et al., 2014), although recent studies using empirical analysis of hydrographic RAPID data dating back to the 1980s show no overall decline (Worthington et al., 2021). Other higher-frequency variations can be found, such as the ∼30% 2009–2010 decrease of AMOC at 26.5°N based on the previous 5 years of measurements (McCarthy et al., 2012). This decrease in strength was detected in the AMOC upper limb at 41°N but not in the deep western return limb at 16°N (MSrokosz & Bryden, 2015; Srokosz et al., 2012).

The relationship between temperature and AMOC enables the use of satellite sea surface temperature as a proxy for long-term reconstructions of AMOC strength (Caesar et al., 2018; Manta et al., 2021), which can be compared to the estimations obtained with global climate numerical models (Caesar et al., 2018; Fraser & Cunningham, 2021). Longer term reconstructions and projections from proxies and high-resolution climate models display a decline in the strength of the AMOC by 15% (Caesar et al., 2018) and 30% (Rahmstorf et al., 2015) since the 1950s, in the frame of a consistent weak AMOC for the last 150 years (Thornalley et al., 2018). Fraser and Cunningham (2021) have found no significant weakening trend in their reconstruction of AMOC over the last 120 years. Expendable bathythermograph (XBT) and Argo profile data enable the estimation of AMOC (Goes et al., 2020; Majumder et al., 2016), and results agree with our inverse model, especially for XBT-derived solutions, with Argo estimates being considerably higher. Monthly XBT transects could complement the study of short-term variability of the AMOC.

3.3. Heat Transport

Total heat transport can be divided into its components attending to the mechanisms of vertical and horizontal circulation, allowing to break up the heat transport into a barotropic (throughflow), baroclinic (overturning), and horizontal (or gyre) component (Bryden & Imawaki, 2001). The throughflow component is the net transport across the section at the section-averaged temperature (Figure S2 in Supporting Information S1); the overturning component is the zonally averaged vertical circulation and the horizontal or gyre component is the horizontal and vertical residual heat (Bryden & Imawaki, 2001; Bryden et al., 2011; McDonagh et al., 2015; Figures 4a, 4c and 4e). Overall, the overturning heat transport (Figure 4c), which represents changes in the meridional structure of the water column, dominates the total heat transport and increases equatorward. The horizontal or gyre

component (Figure 4e) comprises the result of large-scale gyre circulation and eddies, which remains fairly constant across all latitudes and through the decades of this study (McDonagh et al., 2015).

The North Atlantic subtropical gyre (24°N) shows a greater change in terms of overturning heat transport than in the rest of sections, with a strong decrease from a maximum value in 1990–1999 of 1.27 ± 0.06 PW to 0.97 ± 0.07 in 2000–2009 PW and a recovery to 1.10 ± 0.05 PW in 2010–2019. The Labrador Sea (55°N West) net transports are almost null, with negligible contributions from the marked cyclonic gyre affecting the whole basin (Lozier et al., 2019), vertically and horizontally. Nevertheless, in the Eastern subbasin of the northernmost section (55°N East) the overturning component majorly contributes to the total heat transport.

3.4. Freshwater Transport

Oceanic freshwater transport is the non-salt part of mass transport. Its divergence can be understood as the balance of evaporation, precipitation, river runoff, and ice processes. It is calculated by constraining the salt flux across each section to that across the Bering Strait. The salt flux (or non-freshwater part of the mass transport) is not affected by the strength of freshwater divergence as this happens at zero salinity. The freshwater divergence (Figures 4b, 4d and 4f) can be divided, as the heat transport, into its components. On this occasion and in contrast to the heat flux, the freshwater throughflow contributes from 5% to 35% to the total flux (Figure S2 in Supporting Information S1). This component represents the evolution of the section average salinity from that of the Bering Strait (a southward flow of 0.8 Sv with an average salinity of 32.5, resulting in a salinity flux of −26.0 Sv psu; McDonagh & King, 2005; Woodgate & Aagaard, 2005). The freshwater overturning component (Figure 4d) presents a stronger southward transport in the sections close to the equator. The horizontal or gyre freshwater flux (Figure 4f) displays a higher northward freshwater flux in the sections that occupy the subtropical gyres (24 and 36°N in the North Atlantic and 24 and 30°S in the South Atlantic), with similar values for all decades.

The south Atlantic subtropical gyre presents low values of overturning freshwater flux at 30°S, thus being the only section with a horizontal component larger than the overturning (Mecking et al., 2016). Based on our understanding from model studies, the overturning freshwater flux at this latitude has been identified as a possible proxy for the stability of the AMOC (Bryden et al., 2011; De Vries & Weber, 2005; Dijkstra, 2007; Gent, 2018; Rahmstorf, 1996; Weber & Drijfhout, 2007; Weijer et al., 2019), potentially determining whether it is in a monostable or bistable regime. We have found a tendency toward increasingly southward values from 1990 to 1999 (0.00 ± 0.02 Sv) to 2000–2009 (−0.08 ± 0.02 Sv), and no differences within uncertainties between the 2000–2009 decade and the 2010–2019 decade (−0.13 ± 0.03 Sv), with an overall change between 1990–1999 and 2010–2019. Negative values of the overturning freshwater transport at 30°S indicate that the AMOC transports freshwater southwards, and a net input of freshwater north of 30°S is necessary to maintain the salinity structure of the overturning circulation. This result is consistent with other studies relying on observational data that have found that the overturning circulation effectively carries freshwater out of the Atlantic through its southern boundary (Bryden et al., 2011; Garzoli et al., 2013; McDonagh & King, 2005; Saunders & King, 1995; Weijer et al., 1999).

The transport weighted sensitivity of the overturning and horizontal components reflects the change in each component subtracting the effect of a change in the mass transport. The transport weighted freshwater overturning—the freshwater overturning divided by the overturning strength— at 30°S shows a systematic decrease (0.000 ± 0.001, −0.005 ± 0.001, and −0.008 ± 0.002 for each hydrographic cruise done in each decade, respectively) that reflects an increasing difference between the freshwater content in upper and lower layers. To assess the origin of this change, we have computed the transport and area-weighted salinity for upper and thermocline, intermediate, and deep layers. The area-weighted salinity (Figure 4g) values for each layer fail to show changes for each decade. However, the transport-weighted salinity (Figure 4h) for upper and thermocline layers presents higher variability (34.45, 34.68, and 34.96 for the realizations carried out in each decade), whereas the intermediate and deep layers remain fairly constant. Thus, this change in the freshwater overturning arises from an increase in the salinity of upper layers transported northward in the upper ocean, possibly due to higher transport of the salty waters of the Agulhas leakage from the Indian Ocean. Model simulations have indicated that there might be a Southern Hemisphere origin to the AMOC decadal variability arising from the Agulhas leakage (Biastoch et al., 2008). The strength of this variability factor decreases northward but can reach up to 0.6 Sv. On longer timescales, it has shown a correlation with the Atlantic Multidecadal Oscillation, and it has been linked

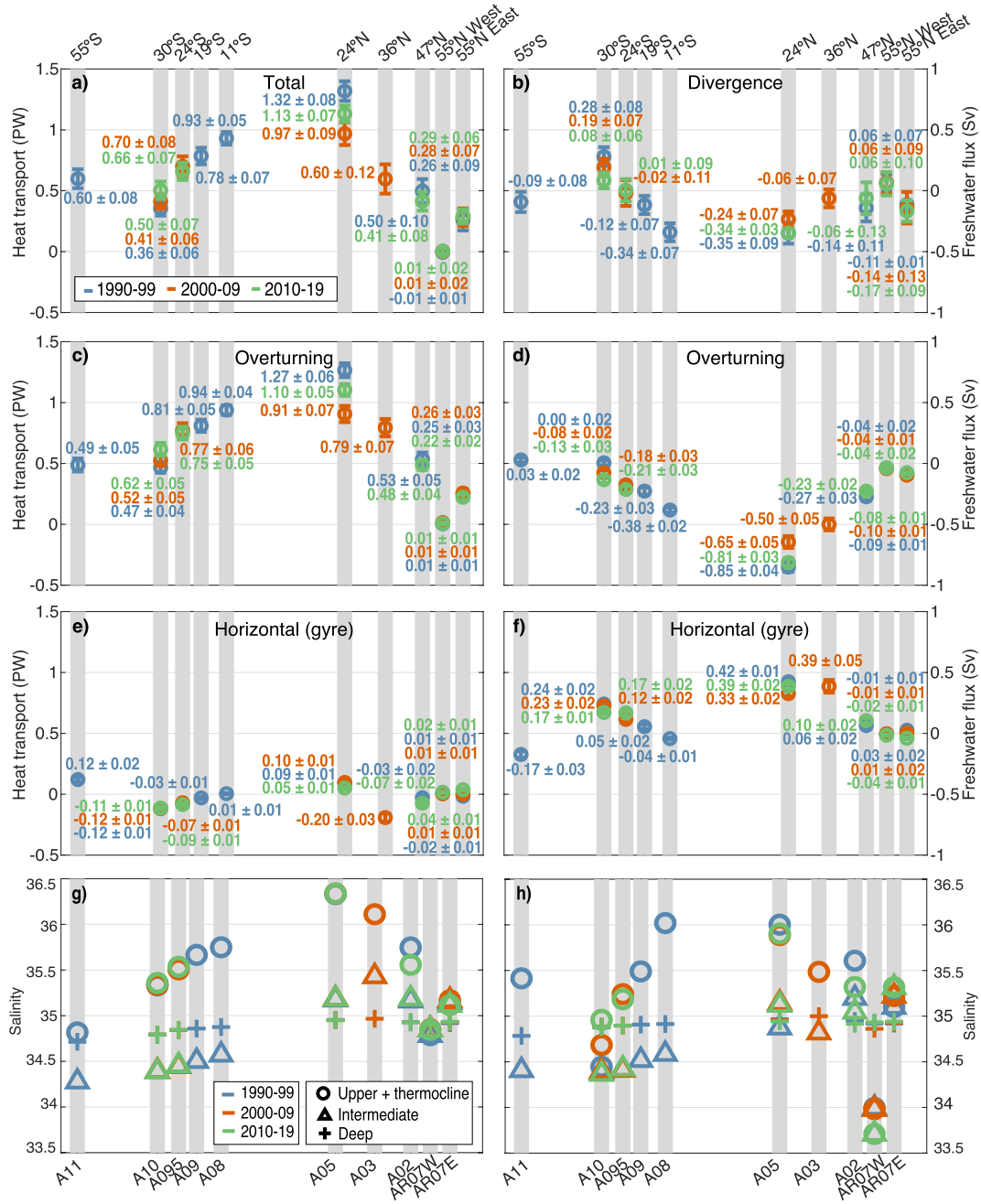

Figure 4. Heat and freshwater transport attending to their components, and area and transport-weighted salinity for each latitude and decade. The gray bars mark the nominal latitude of each zonal section, and the colors represent each decade, blue for 1990–1999, orange for 2000–2009, and green for 2010–2019. The left panels (a, c, and e) are the heat transport in PW, and the panels on the right (b, d, and f) are the freshwater transport in Sv. The total transport (a) and (b) is divided in throughflow, overturning (c) and (d), and horizontal or gyre (e) and (f). The total heat transport (a) is similar to the overturning heat transport (c), as the horizontal component (e) is quite small. The freshwater divergence (b) also looks like the overturning component (d), but the horizontal (f) component cannot be neglected. The higher variability among decades appears at 24°N in both property fluxes for the overturning component. There is an increase in northward heat transport and southward freshwater transport equatorward. The uncertainties associated with the heat and freshwater transports are part of the results of the inverse model solved using the Gauss-Markov estimator. The bottom panels are the area-weighted (g) and transport-weighted salinity (h). Each property has been divided into three water masses – upper and thermocline waters (circles), intermediate waters (triangles), and deep waters (crosses). The area-weighted salinity (g) does not show any decadal changes for any water masses, although the transport-weighted salinity (h) manifests an increasing trend at 30°S for the upper and thermocline waters. As a result, the stratification in the water column is stronger, reflected in the higher values of the overturning component of freshwater.

to wind-driven processes (Biastoch et al., 2015). Other studies have found no significant impact on the AMOC (Weijer & van Sebille, 2014), and therefore, a discussion on this topic continues.

4. Conclusions

The behavior of the AMOC and its driving mechanisms and feedbacks have received much attention in climate change scenarios due to the major climate impacts associated with a predicted slowdown. As a result, several ocean locations are being monitored to estimate the changes in the strength of the AMOC at different latitudes.

Our results from inverse models based on hydrographic data show that the Atlantic basin overturning transport displays no changes at any latitude between the different hydrographic cruises. In the SPNA, our results indicate that the major contributor to the AMOC for the three decades is the Eastern basin (55°N East) as estimated by OSNAP for the last decade.

At 30°S, an increase of southward freshwater overturning transport has been estimated over the three decades, indicating that the AMOC is possibly in a bistable state based on findings from model studies. These negative values appear when AMOC exports freshwater out of the Atlantic, equivalent to a net precipitation over the Atlantic basin. In this case, the AMOC has multiple equilibria and may collapse due to a large enough freshwater perturbation (Dijkstra, 2007; Mecking et al., 2016; Weijer et al., 2019).

Data Availability Statement

Hydrographic data were collected from the CCHDO website (https://cchdo.ucsd.edu) in the frame of International WOCE and GO-SHIP projects and from the BODC databases for each cruise: A11 1992 (https://cchdo.ucsd.edu/cruise/74DI199_1), A10 1992 (https://cchdo.ucsd.edu/cruise/06MT22_5), A09 1991 (https://cchdo.ucsd.edu/cruise/06MT15_3), A08 1994 (https://cchdo.ucsd.edu/cruise/06MT28_1), A05 1992 (https://cchdo.ucsd.edu/cruise/29HE06_1), A02 1993 (https://cchdo.ucsd.edu/cruise/06GA226_2), AR07 W 1990 (https://cchdo.ucsd.edu/cruise/18DA90012_1), AR07 E 1991 (https://cchdo.ucsd.edu/cruise/74AB62_1), A10 2003 (https://cchdo.ucsd.edu/cruise/49NZ20031106), A095 2009 (https://cchdo.ucsd.edu/cruise/740H20090307), A05 2004 (https://cchdo.ucsd.edu/cruise/74DI20040404), A03 2005 (https://www.bodc.ac.uk/data/bodc_database/ctd/search/, searching for 36 North under 'Project'), AR07 W 2005 (https://cchdo.ucsd.edu/cruise/18HU20050526), AR07 E 2007 (https://cchdo.ucsd.edu/cruise/64PE20070830), A10 2011 (https://cchdo.ucsd.edu/cruise/33RO20110926), A095 2018 (https://cchdo.ucsd.edu/cruise/740H20180228), A05 2011 (https://cchdo.ucsd.edu/cruise/29AH20110128), A02 2013 (https://cchdo.ucsd.edu/cruise/06M220130509), AR07 W 2014 (https://cchdo.ucsd.edu/cruise/74JC20140606) and AR07 E 2014 (https://cchdo.ucsd.edu/cruise/74JC20140606). OSNAP data were collected and made freely available by the OSNAP project and all the national programs that contribute to it (https://www.o-snap.org/). Data from the full OSNAP array for the first 21 months (31-Jul-2014 to 20-Apr-2016) have been used to produce the 30-day mean MOC, MHT, and MFT time series across the whole section, as well as the gridded property fields, and are available at https://doi.org/10.35090/wa93-m688. Data from the RAPID-MOCHA program are funded by the U.S. National Science Foundation and UK Natural Environment Research Council. MOC data from the RAPID-MOCHA are freely available at https://rapid.ac.uk/rapidmoc/rapid_data/datadl.php (doi:10/d3z4) and heat transports at https://mocha.rsmas.miami.edu/mocha/results/index.html (doi:10/gwqg). The Florida Current cable and section data are made freely available on the Atlantic Oceanographic and Meteorological Laboratory web page (www.aoml.noaa.gov/phod/floridacurrent/) and are funded by the DOC-NOAA Climate Program Office - Ocean Observing and Monitoring Division. Florida Current daily mean transport from year 2000 until present is available at https://www.aoml.noaa.gov/phod/floridacurrent/data_access.php and historical data from 1982 to 1998 at https://www.aoml.noaa.gov/phod/floridacurrent/historical_data.php, of which we have used the used data from 1990 to 1998. The daily mean u and v-wind components of NCEP/NCAR reanalysis winds were collected from https://psl.noaa.gov/data/gridded/data.ncep.reanalysis.pressure.html.

Acknowledgments
We thank the chief scientists and teams that collected all the data for the zonal sections: P. Saunders, T. Müller, G. Siedler, G. Parrilla, A. Sy, J. Lazier, M. Bersch, Y. Yoshikawa, B. King, S. Cunningham, G. Harrison, G. J.Brummer, M. Baringer, A. Macdonald, D. Kieke, and P. Holliday. This article is a publication of the Unidad Océano y Clima from Universidad de Las Palmas de Gran Canaria, an R&D&i CSIC-associate unit. This work has been completed as part of V.C. work at IOCAG, in the doctoral program in Oceanography and Global Change. V.C. acknowledges the Agencia Canaria de Investigación, Innovación y Sociedad de la Información (ACIISI) grant program of "Apoyo al personal investigador en formación" TESIS2019010015, as well as NORCE for hosting a guest student to develop the study. M.D.P.-H. would like to thank the support of the "Programa Postdoctoral de la Universidad de Las Palmas de Gran Canaria". This study was supported by the SAGA project (RTI2018-100844-B-C31) funded by the Ministerio de Ciencia, Innovación y Universidades of the Spanish Government. This study was additionally supported by the TRIATLAS project, which has received funding from the European Union's Horizon 2020 research and innovation programme under grant agreement No 817578.

References

Baringer, M. O., & Molinari, R. (1999). Atlantic Ocean baroclinic heat flux at 24 to 26°N. *Geophysical Research Letters*, *26*(3), 353–356. https://doi.org/10.1029/1998gl900323

Biastoch, A., Böning, C. W., & Lutjeharms, J. R. E. (2008). Agulhas leakage dynamics affects decadal variability in Atlantic overturning circulation. *Nature*, *456*(7221), 489–492. https://doi.org/10.1038/nature07426

Biastoch, A., Durgadoo, J. V., Morrison, A. K., van Sebille, E., Weijer, W., & Griffies, S. M. (2015). Atlantic multi-decadal oscillation covaries with Agulhas leakage. *Nature Communications*, *6*(1), 10082. https://doi.org/10.1038/ncomms10082

Bryden, H. L., & Imawaki, S. (2001). Chapter 6.1 Ocean heat transport. In G. Siedler, J. Church, & J. Gould (Eds.), *ocean circulation & climate: Observing and modelling the global ocean* (pp. 455–474). Academic Press. https://doi.org/10.1016/S0074-6142(01)80134-0

Bryden, H. L., King, B. A., & McCarthy, G. D. (2011). South Atlantic overturning circulation at 24°S. *Journal of Marine Research*, *69*(1), 39–55. https://doi.org/10.1357/002224011798147633

Bryden, H. L., Longworth, H. R., & Cunningham, S. A. (2005). Slowing of the Atlantic meridional overturning circulation at 25°N. *Nature*, *438*, 655–657. https://doi.org/10.1038/nature04385

Caesar, L., McCarthy, G. D., Thornalley, D. J. R., Cahill, N., & Rahmstorf, S. (2021). Current Atlantic meridional overturning circulation weakest in last millennium. *Nature Geoscience*, *14*(3), 1–120. https://doi.org/10.1038/s41561-021-00699-z

Caesar, L., Rahmstorf, S., Robinson, A., Feulner, G., & Saba, V. (2018). Observed fingerprint of a weakening Atlantic Ocean overturning circulation. *Nature*, *556*(7700), 191–196. https://doi.org/10.1038/s41586-018-0006-5

Cunningham, S. A., Kanzow, T., Rayner, D., Baringer, M. O., Johns, W. E., & Marotzke, J. (2007). Temporal variability of the Atlantic meridional overturning circulation at 26.5°N. *Science*, *317*, 935–938. https://doi.org/10.1126/science.1141304

de Vries, P., & Weber, S. L. (2005). The Atlantic freshwater budget as a diagnostic for the existence of a stable shut down of the meridional overturning circulation. *Geophysical Research Letters*, *32*(9), L09606. https://doi.org/10.1029/2004GL021450

Desbruyères, D. G., Mercier, H., Maze, G., & Daniault, N. (2019). Surface predictor of overturning circulation and heat content change in the subpolar North Atlantic. *Ocean Science*, *15*(3), 809–817. https://doi.org/10.5194/os-15-809-2019

Dijkstra, H. A. (2007). Characterization of the multiple equilibria regime in a global ocean model. *Tellus*, *59A*, 695–705. https://doi.org/10.1111/j.1600-0870.2007.00267.x

Frajka-Williams, E., Ansorge, I. J., Baehr, J., Bryden, H. L., Chidichimo, M. P., Cunningham, S. A., et al. (2019). Atlantic meridional overturning circulation: Observed transport and variability. *Frontiers in Marine Science*, *6*(260). https://doi.org/10.3389/fmars.2019.00260

Fraser, N. J., & Cunningham, S. A. (2021). 120 Years of AMOC variability reconstructed from observations using the Bernoulli inverse. *Geophysical Research Letters*, *48*(18). https://doi.org/10.1029/2021GL093893

Fu, Y., Karstensen, J., & Brandt, P. (2018). Atlantic meridional overturning circulation at 14.5°N in 1989 and 2013 and 24.5°N in 1992 and 2015: Volume, heat, and freshwater transports. *Ocean Science*, 589–616. https://doi.org/10.5194/os-14-589-2018

Fu, Y., Li, F., Karstensen, J., & Wang, C. (2020). A stable Atlantic meridional overturning circulation in a changing North Atlantic ocean since the 1990s. *Science Advances*, *6*(48), eabc7836. https://doi.org/10.1126/sciadv.abc7836

Ganachaud, A. S. (2003b). Large-scale mass transports, water mass formation, and diffusivities estimated from World Ocean Circulation Experiment (WOCE) hydrographic data. *Journal of Geophysical Research*, *108*(C7). https://doi.org/10.1029/2002jc001565

Ganachaud, A. S., & Wunsch, C. (2000). Improved estimates of global ocean circulation, heat transport and mixing from hydrographic data. *Nature*, *408*, 453–456. https://doi.org/10.1038/35044048

Ganachaud, A. S., & Wunsch, C. (2003). Large-scale ocean heat and freshwater transports during the world ocean circulation experiment. *Journal of Climate*, *16*, 696–705. https://doi.org/10.1175/1520-0442(2003)016<0696:LSOHAF>2.0.CO;2

Garzoli, S. L., Baringer, M. O., Dong, S., Perez, R. C., & Yao, Q. (2013). South Atlantic meridional fluxes. *Deep-Sea Research Part I Oceanographic Research Papers*, *71*, 21–32. https://doi.org/10.1016/j.dsr.2012.09.003

Gent, P. R. (2018). A commentary on the Atlantic meridional overturning circulation stability in climate models. *Ocean Modelling*, *122*, 57–66. https://doi.org/10.1016/j.ocemod.2017.12.006

Goes, M., Goni, G., Dong, S., Boyer, T., & Baringer, M. (2020). The complementary value of XBT and Argo observations to monitor ocean boundary currents and meridional heat and volume transports: A case study in the Atlantic Ocean. *Journal of Atmospheric and Oceanic Technology*, *37*(12), 2267–2282. https://doi.org/10.1175/JTECH-D-20-0027.1

Hernández-Guerra, A., Pelegrí, J. L., Fraile-Nuez, E., Benítez-Barrios, V. M., Emelianov, M., Pérez-Hernández, M. D., & Vélez-Belchí, P. (2014). Meridional overturning transports at 7.5°N and 24.5°N in the Atlantic Ocean during 1992–93 and 2010–11. *Progress in Oceanography*, *128*, 98–114. https://doi.org/10.1016/j.pocean.2014.08.016

Hernández-Guerra, A., & Talley, L. D. (2016). Meridional overturning transports at 30°S in the Indian and Pacific oceans in 2002–2003 and 2009. *Progress in Oceanography*, *146*, 89–120. https://doi.org/10.1016/j.pocean.2016.06.005

Hernández-Guerra, A., Talley, L. D., Pelegrí, J. L., Vélez-Belchí, P., Baringer, M. O., Macdonald, A. M., & McDonagh, E. L. (2019). The upper, deep, abyssal and overturning circulation in the Atlantic Ocean at 30°S in 2003 and 2011. *Progress in Oceanography*, *176*. https://doi.org/10.1016/j.pocean.2019.102136

Hummels, R., Brandt, P., Dengler, M., Fischer, J., Araujo, M., Veleda, D., & Durgadoo, J. V. (2015). Interannual to decadal changes in the western boundary circulation in the Atlantic at 11°S. *Geophysical Research Letters*, *42*(18), 7615–7622. https://doi.org/10.1002/2015GL065254

Jackett, D. R., & McDougall, T. J. (1997). A neutral density variable for the World's Oceans. *Journal of Physical Oceanography*, *27*(2), 237–263. https://doi.org/10.1175/1520-0485(1997)027<0237:ANDVFT>2.0.CO;2

Johns, W. E., Baringer, M. O., Beal, L. M., Cunningham, S. A., Kanzow, T., Bryden, H. L., et al. (2011). Continuous, array-based estimates of Atlantic Ocean heat transport at 26.5°N. *Journal of Climate*, *24*, 2429–2449. https://doi.org/10.1175/2010JCLI3997.1

Kanzow, T., Send, U., Zenk, W., Chave, A. D., & Rhein, M. (2006). Monitoring the integrated deep meridional flow in the tropical North Atlantic: Long-term performance of a geostrophic array. *Deep-Sea Research Part I Oceanographic Research Papers*, *53*(3), 528–546. https://doi.org/10.1016/j.dsr.2005.12.007

Kersalé, M., Meinen, C. S., Perez, R. C., Le Hénaff, M., Valla, D., Lamont, T., et al. (2020). Highly variable upper and abyssal overturning cells in the South Atlantic. *Science Advances*, *6*(32), eaba7573. https://doi.org/10.1126/sciadv.aba7573

Koltermann, K. P., Sokov, A. V., Tereschenkov, V. P., Dobroliubov, S. A., Lorbacher, K., & Sy, A. (1999). Decadal changes in the thermohaline circulation of the North Atlantic. *Deep-Sea Research Part II Topical Studies in Oceanography*, *46*(1–2), 109–138. https://doi.org/10.1016/S0967-0645(98)00115-5

Lozier, M. S., Bacon, S., Bower, A. S., Cunningham, S. A., de Jong, M. F., Steur, L. de, et al. (2017). Overturning in the subpolar North Atlantic program: A new international Ocean Observing system. *Bulletin of the American Meteorological Society*, *98*(4), 737–752. https://doi.org/10.1175/bams-d-16-0057.1

Lozier, M. S., Li, F., Bacon, S., Bahr, F., Bower, A. S., Cunningham, S. A., et al. (2019). A sea change in our view of overturning in the subpolar North Atlantic. *Science*, *363*(6426), 516–521. https://doi.org/10.1126/science.aau6592

Lumpkin, R., & Speer, K. G. (2007). Global Ocean meridional overturning. *Journal of Physical Oceanography*, *37*(10), 2550–2562. https://doi.org/10.1175/jpo3130.1

Macdonald, A. M. (1995). *Ocean fluxes of mass, heat and freshwater: A global estimate and perspective*. Massachusetts Institute of Technology & Woods Hole Oceanographic Institution. https://doi.org/10.1575/1912/5620

Majumder, S., Schmid, C., & Halliwell, G. (2016). An observations and model-based analysis of meridional transports in the South Atlantic. *Journal of Geophysical Research: Oceans*, *121*. https://doi.org/10.1002/2016jc011693

Manta, G., Speich, S., Karstensen, J., Hummels, R., Kersalé, M., Laxenaire, R., et al. (2021). The South Atlantic meridional overturning circulation and mesoscale eddies in the first GO-SHIP section at 34.5°S. *Journal of Geophysical Research: Oceans*, *126*(2), 1–25. https://doi.org/10.1029/2020JC016962

McCarthy, G., Frajka-Williams, E., Johns, W. E., Baringer, M. O., Meinen, C. S., Bryden, H. L., et al. (2012). Observed interannual variability of the Atlantic meridional overturning circulation at 26.5°N. *Geophysical Research Letters*, *39*, L19609. https://doi.org/10.1029/2012GL052933

McCarthy, G. D., Brown, P. J., Flagg, C. N., Goni, G., Houpert, L., Hughes, C. W., et al. (2020). Sustainable observations of the AMOC: Methodology and technology. *Reviews of Geophysics*, *58*(1), 1–34. https://doi.org/10.1029/2019RG000654

McCartney, M. S., & Talley, L. D. (1984). Warm-to-cold water conversion in the northern North Atlantic Ocean. *Journal of Physical Oceanography*, *14*, 922–935. https://doi.org/10.1175/1520-0485(1984)014<0922:wtcwci>2.0.co;2

McDonagh, E. L., & King, B. A. (2005). Oceanic fluxes in the south Atlantic. *Journal of Physical Oceanography*, *35*(1), 109–122. https://doi.org/10.1175/JPO-2666.1

McDonagh, E. L., King, B. A., Bryden, H. L., Courtois, P., Szuts, Z., Baringer, M. O., et al. (2015). Continuous estimate of Atlantic oceanic freshwater flux at 26.5°N. *Journal of Climate*, *28*, 8888–8906. https://doi.org/10.1175/jcli-d-14-00519.1

Mecking, J. V., Drijfhout, S. S., Jackson, L. C., & Graham, T. (2016). Stable AMOC off state in an eddy-permitting coupled climate model. *Climate Dynamics*, *47*(7–8), 2455–2470. https://doi.org/10.1007/s00382-016-2975-0

Meinen, C. S., Speich, S., Perez, R. C., Dong, S., Piola, A. R., Garzoli, S. L., et al. (2013). Temporal variability of the meridional overturning circulation at 34.5°S: Results from two pilot boundary arrays in the South Atlantic. *Journal of Geophysical Research: Oceans*, *118*(12), 6461–6478. https://doi.org/10.1002/2013JC009228

Moat, B. I., Smeed, D. A., Frajka-Williams, E., Desbruyères, D. G., Beaulieu, C., Johns, W. E., et al. (2020). Pending recovery in the strength of the meridional overturning circulation at 26° N. *Ocean Science*, *16*(4), 863–874. https://doi.org/10.5194/os-16-863-2020

Petit, T., Lozier, M. S., Josey, S. A., & Cunningham, S. A. (2020). Atlantic deep water formation occurs primarily in the Iceland Basin and Irminger Sea by local buoyancy forcing. *Geophysical Research Letters*, *47*(22), 1–9. https://doi.org/10.1029/2020GL091028

Rahmstorf, S. (1996). On the freshwater forcing and transport of the Atlantic thermohaline circulation. *Climate Dynamics*, *12*, 799–811. https://doi.org/10.1007/s003820050144

Rahmstorf, S., Box, J. E., Feulner, G., Mann, M. E., Robinson, A., Rutherford, S., & Schaffernicht, E. J. (2015). Exceptional twentieth-century slowdown in Atlantic Ocean overturning circulation. *Nature Climate Change*, *5*(5), 475–480. https://doi.org/10.1038/nclimate2554

Roberts, C. D., Jackson, L., & McNeall, D. (2014). Is the 2004-2012 reduction of the Atlantic meridional overturning circulation significant? *Geophysical Research Letters*, *41*(9), 3204–3210. https://doi.org/10.1002/2014GL059473

Saunders, P. M., & King, B. A. (1995). Oceanic fluxes on the WOCE A11 section. *Journal of Physical Oceanography*, *25*, 1942–1958. https://doi.org/10.1175/1520-0485(1995)025<1942:ofotwa>2.0.co;2

Sévellec, F., & Sinha, B. (2018). Predictability of decadal Atlantic meridional overturning circulation variations. *Oxford Encyclopedia of Climate Science*. https://doi.org/10.1093/acrefore/9780190228620.013.81.hal-02136510

Sloyan, B. M., & Rintoul, S. R. (2001). The Southern Ocean limb of the global deep overturning circulation. *Journal of Physical Oceanography*, *31*(1), 143–173. https://doi.org/10.1175/1520-0485(2001)031<0143:tsolot>2.0.co;2

Srokosz, M., Baringer, M., Bryden, H., Cunningham, S., Delworth, T., Lozier, S., et al. (2012). Past, present, and future changes in the Atlantic meridional overturning circulation. *Bulletin of the American Meteorological Society*, *93*(11), 1663–1676. https://doi.org/10.1175/BAMS-D-11-00151.1

Srokosz, M. A., & Bryden, H. L. (2015). Observing the Atlantic meridional overturning circulation yields a decade of inevitable surprises. *Science*, *348*(6241). https://doi.org/10.1126/science.1255575

Talley, L. D. (2008). Freshwater transport estimates and the global overturning circulation: Shallow, deep and throughflow components. *Progress in Oceanography*, *78*(4), 257–303. https://doi.org/10.1016/j.pocean.2008.05.001

Talley, L. D., Feely, R. A., Sloyan, B. M., Wanninkhof, R., Baringer, M. O., Bullister, J. L., et al. (2016). Changes in ocean heat, carbon content, and ventilation: A review of the first decade of GO-SHIP global repeat hydrography. *Annual Review of Marine Science*, *8*(1), 185–215. https://doi.org/10.1146/annurev-marine-052915-100829

Thornalley, D. J. R., Oppo, D. W., Ortega, P., Robson, J. I., Brierley, C. M., Davis, R. E., et al. (2018). Anomalously weak Labrador Sea convection and Atlantic overturning during the past 150 years. *Nature*, *556*(7700), 227–230. https://doi.org/10.1038/s41586-018-0007-4

Weber, S. L., & Drijfhout, S. S. (2007). Stability of the Atlantic meridional overturning circulation in the last glacial maximum climate. *Geophysical Research Letters*, *34*(22), L22706. https://doi.org/10.1029/2007GL031437

Wefer, G., Berger, W. H., Siedler, G., & Webb, D. J. (1996). In G. Wefer, W. H. Berger, G. Siedler, & D. J. Webb (Eds.), *The South Atlantic: Present and past circulation*. Springer.

Weijer, W., Cheng, W., Drijfhout, S. S., Fedorov, A. V., Hu, A., Jackson, L. C., et al. (2019). Stability of the Atlantic meridional overturning circulation: A review and synthesis. *Journal of Geophysical Research: Oceans*, *124*(8), 5336–5375. https://doi.org/10.1029/2019JC015083

Weijer, W., de Ruijter, W. P. M., Dijkstra, H. A., & van Leeuwen, P. J. (1999). Impact of interbasin exchange on the Atlantic overturning circulation. *Journal of Physical OceanographyCO*, *29*(9), 2266–2284. https://doi.org/10.1175/1520-0485(1999)029<2266:ioieot>2.0.co;2

Weijer, W., & van Sebille, E. (2014). Impact of Agulhas leakage on the Atlantic overturning circulation in the CCSM4. *Journal of Climate*, *27*(1), 101–110. https://doi.org/10.1175/JCLI-D-12-00714.1

Woodgate, R. A., & Aagaard, K. (2005). Revising the Bering Strait freshwater flux into the Arctic ocean. *Geophysical Research Letters*, *32*. https://doi.org/10.1029/2004GL021747

Worthington, E. L., Moat, B. I., Smeed, D. A., Mecking, J. V., Marsh, R., & McCarthy, G. D. (2021). A 30-year reconstruction of the Atlantic meridional overturning circulation shows no decline. *Ocean Science*, *17*(1), 285–299. https://doi.org/10.5194/os-17-285-2021

Wunsch, C. (1978). The North Atlantic general circulation west of 50°W determined by inverse methods. *Reviews of Geophysics and Space Physics*, *16*(4), 583–620. https://doi.org/10.1029/rg016i004p00583

Wunsch, C. (1996). *The ocean circulation inverse problem*. Cambridge University Press.

References From the Supporting Information

Artana, C., Ferrari, R., Koenig, Z., Sennéchael, N., Saraceno, M., Piola, A. R., & Provost, C. (2018). Malvinas current volume transport at 41°S: A 24 yearlong time series consistent with mooring data from 3 decades and satellite altimetry. *Journal of Geophysical Research: Oceans*, *123*(1), 378–398. https://doi.org/10.1002/2017JC013600

Bersch, M., Yashayaev, I., & Koltermann, K. P. (2007). Recent changes of the thermohaline circulation in the subpolar North Atlantic. *Ocean Dynamics*, *57*(3), 223–235. https://doi.org/10.1007/s10236-007-0104-7

Curry, B., Lee, C. M., Petrie, B., Moritz, R. E., & Kwok, R. (2014). Multiyear volume, liquid freshwater, and sea ice transports through Davis Strait, 2004–10. *Journal of Physical Oceanography*, *44*(4), 1244–1266. https://doi.org/10.1175/jpo-d-13-0177.1

Ganachaud, A. S. (1999). *Large scale oceanic circulation and fluxes of freshwater, heat, nutrients and oxygen*. Massachusetts Institute of Technology and Woods Hole Oceanographic Institution. https://doi.org/10.1575/1912/4130

Ganachaud, A. S. (2003a). Error budget of inverse box models: The North Atlantic. *Journal of Atmospheric and Oceanic Technology*, *20*(11), 1641–1655. https://doi.org/10.1175/1520-0426(2003)020<1641:EBOIBM>2.0.CO;2

Hogg, N., Biscaye, P., Gardner, W., & Schmitz, W. J. (1982). On the transport and modification of Antarctic bottom water in the Vema channel. *Journal of Marine Research*, *40*, 231–263.

Hogg, N. G., & Owens, W. B. (1999). Direct measurement of the deep circulation within the Brazil Basin. *Deep Sea Research Part II: Topical Studies in Oceanography*, *46*(1–2), 335–353. https://doi.org/10.1016/S0967-0645(98)00097-6

Holliday, N. P., Bacon, S., Cunningham, S. A., Gary, S. F., Karstensen, J., King, B. A., et al. (2018). Subpolar North Atlantic overturning and gyre-scale circulation in the summers of 2014 and 2016. *Journal of Geophysical Research: Oceans*, *123*(7), 4538–4559. https://doi.org/10.1029/2018JC013841

Katsumata, K., & Fukasawa, M. (2011). Changes in meridional fluxes and water properties in the Southern Hemisphere subtropical oceans between 1992/1995 and 2003/2004. *Progress in Oceanography*, *89*(1–4), 61–91. https://doi.org/10.1016/j.pocean.2010.12.008

King, B. A., Sanchez-Franks, A., & Firing, Y. L. (2019). *RRS james cook cruise JC159 28 February - 11 April 2018. Hydrographic sections from the Brazil to the Benguela current across 24S in the Atlantic*, 60, (pp. 193). National Oceanography Centre Cruise Report.

Lazier, J., Hendry, R., Clarke, A., Yashayaev, I., & Rhines, P. (2002). Convection and restratification in the Labrador Sea, 1990–2000. *Deep Sea Research Part I: Oceanographic Research Papers*, *49*(10), 1819–1835. https://doi.org/10.1016/S0967-0637(02)00064-X

Lozier, M. S., Li, F., Bacon, S., Bahr, F., Bower, A. S., Cunningham, S. A., et al. (2019). *Meridional overturning circulation and the associated heat and freshwater transports observed by the OSNAP (Overturning in the Subpolar North Atlantic Program) array from 2014 to 2016*. Duke Digital Repository. https://doi.org/10.7924/r4z60gf0f

McDonagh, E. L., Bryden, H. L., King, B. A., & Sanders, R. J. (2008). The circulation of the Indian Ocean at 32°S. *Progress in Oceanography*, *79*(1), 20–36. https://doi.org/10.1016/j.pocean.2008.07.001

McDonagh, E. L., McLeod, P., King, B. A., Bryden, H. L., & Torres Valdés, S. (2010). Circulation, heat, and freshwater transport at 36°N in the Atlantic. *Journal of Physical Oceanography*, *40*(12), 2661–2678. https://doi.org/10.1175/2010JPO4176.1

Moat, B. I., Josey, S. A., Sinha, B., Blaker, A. T., Smeed, D. A., McCarthy, G. D., et al. (2016). Major variations in subtropical North Atlantic heat transport at short (5 day) timescales and their causes. *Journal of Geophysical Research: Oceans*, *121*(5), 3237–3249. https://doi.org/10.1002/2016JC011660

Morris, M. Y., Hall, M. M., St Laurent, L. C., & Hogg, N. G. (2001). Abyssal mixing in the Brazil basin. *Journal of Physical Oceanography*, *31*(11), 3331–3348. https://doi.org/10.1175/1520-0485(2001)031<3331:AMITBB>2.0.CO;2

Munk, W. H. (1966). Abyssal recipes. *Deep-Sea Research*, *13*, 707–730. https://doi.org/10.1016/0011-7471(66)90602-4

Parrilla, G., Lavín, A., Bryden, H. L., García, M., & Millard, R. (1994). Rising temperatures in the subtropical North Atlantic Ocean over the past 35 years. *Nature*, *369*(6475), 48–51. https://doi.org/10.1038/369048a0

Rhein, M., Mertens, C., & Roessler, A. (2019). Observed transport decline at 47°N, western Atlantic. *Journal of Geophysical Research: Oceans*, *124*, 4875–4890. https://doi.org/10.1029/2019jc014993

Robbins, P. E., & Toole, J. M. (1997). The dissolved silica budget as a constraint on the meridional overturning circulation of the Indian Ocean. *Deep Sea Research Part I: Oceanographic Research Papers*, *44*(5), 879–906. https://doi.org/10.1016/S0967-0637(96)00126-4

Siedler, G., Müller, T. J., Onken, R., Arhan, M., Mercier, H., King, B. A., & Saunders, P. M. (1996). The zonal WOCE sections in the south Atlantic. In G. Wefer, W. H. Berger, G. Siedler, & D. J. Webb (Eds.), *The South Atlantic: Present and past circulation* (pp. 83–104). Springer-Verlag. https://doi.org/10.1007/978-3-642-80353-6_5

Speer, K. G., Holfort, J., Reynaud, T., & Siedler, G. (1996). South Atlantic heat transport at 11°S. In *The South Atlantic: Present and past circulation* (pp. 105–120). https://doi.org/10.1007/978-3-642-80353-6_6

Toole, J. M., Curry, R., Joyce, T. M., McCartney, M., & Peña-Molino, B. (2011). Transport of the north Atlantic deep western boundary current about 39°N, 70°W: 2004-2008. *Deep-Sea Research Part II*, *58*, 1768–1780. https://doi.org/10.1016/j.dsr2.2010.10.058

Våge, K., Pickart, R. S., Spall, M. A., Valdimarsson, H., Jónsson, S., Torres, D. J., et al. (2011). Significant role of the North Icelandic Jet in the formation of Denmark Strait overflow water. *Nature Geoscience*, *4*, 723–727. https://doi.org/10.1038/ngeo1234

Warren, B. A., & Speer, K. G. (1991). Deep circulation in the eastern south Atlantic Ocean. *Deep Sea Research Part A. Oceanographic Research Papers*, *38*, S281–S322. https://doi.org/10.1016/s0198-0149(12)80014-8

Woodgate, R. A. (2018). Increases in the Pacific inflow to the Arctic from 1990 to 2015, and insights into seasonal trends and driving mechanisms from year-round Bering Strait mooring data. *Progress in Oceanography*, *160*, 124–154. https://doi.org/10.1016/j.pocean.2017.12.007

Woodgate, R. A., Aagaard, K., & Weingartner, T. J. (2005). Monthly temperature, salinity, and transport variability of the Bering Strait through flow. *Geophysical Research Letters*, *32*(4). https://doi.org/10.1029/2004GL021880

Yashayaev, I., & Loder, J. W. (2016). Recurrent replenishment of Labrador Sea Water and associated decadal-scale variability. *Journal of Geophysical Research: Oceans*, *121*(11), 8095–8114. https://doi.org/10.1002/2016JC012046

Yashayaev, I., & Loder, J. W. (2017). Further intensification of deep convection in the Labrador Sea in 2016. *Geophysical Research Letters*, *44*, 1429–1438. https://doi.org/10.1002/2016GL071668